

Received: 2020.09.07  
Accepted: 2020.12.16  
Available online: 2020.12.31  
Published: 2021.03.03

# A Network Pharmacology Study of the Molecular Mechanisms of *Hypericum japonicum* in the Treatment of Cholestatic Hepatitis with Validation in an Alpha-Naphthylisothiocyanate (ANIT) Hepatotoxicity Rat Model

Authors' Contribution:  
Study Design A  
Data Collection B  
Statistical Analysis C  
Data Interpretation D  
Manuscript Preparation E  
Literature Search F  
Funds Collection G

ACE 1 **Sen Ling Feng\***  
BCEF 2 **Jing Zhang\***  
BC 1 **Hongliu Jin**  
BC 1 **Wen Ting Zhu**  
ABCDEF 1 **Zhongwen Yuan**

1 Department of Pharmacy, The Third Affiliated Hospital of Guangzhou Medical University, Guangzhou, Guangdong, P.R. China  
2 Department of Pharmacy, Guangzhou Eighth People's Hospital, Guangzhou Medical University, Guangzhou, Guangdong, P.R. China

\* Sen Ling Feng, Jing Zhang contributed equally  
Zhongwen Yuan, e-mail: zhwyuan1985@163.com

**Corresponding Author:**

**Source of support:**

This work was supported by the National Natural Science Foundation of China (No.81803689), the Natural Science Foundation of Guangdong Province (No.2018A030310292), and The Third Affiliated Hospital of Guangzhou Medical University scientific research project (No.2017B05)

**Background:** This network pharmacology study aimed to identify the active compounds and molecular mechanisms involved in the effects of *Hypericum japonicum* on cholestatic hepatitis. We validated the findings in an alpha-naphthylisothiocyanate (ANIT) rat model of hepatotoxicity.





**Material/Methods:** The chemical constituents and targets of *H. japonicum* and target genes previously associated with cholestatic hepatitis were retrieved from public databases. A network was constructed using Cytoscape 3.7.2 software and the STRING database and potential protein functions were analyzed based on the public platform of bioinformatics. ANIT was used to induce cholestatic hepatitis in a rat model using 36 Sprague-Dawley rats, and this model was used to investigate intervention with 3 doses of quercetin (low-dose, 50 mg/kg; medium-dose, 100 mg/kg; and high-dose, 200 mg/kg), the main active component of *H. japonicum*. Levels of serum biochemical indexes were measured by commercial kits, and the messenger RNA (mRNA) levels of markers of liver and mitochondrial function and oxidative stress were detected by real-time reverse transcription-polymerase chain reaction (RT-PCR).

**Results:** The main active ingredients of *H. japonicum* were quercetin, kaempferol, and tetramethoxyluteolin, and their key targets included prostaglandin G/H synthase 2 (PTGS2), B-cell lymphoma-2 (BCL2), cholesterol 7-alpha hydroxylase (CYP7A1), and farnesoid X receptor (FXR). Quercetin intervention promoted recovery from cholestatic hepatitis.

**Conclusions:** The findings from this research provide support for future research on the roles of quercetin, kaempferol, and tetramethoxyluteolin in human liver disease and the roles of the PTGS2, BCL2, CYP7A1, and FXR genes in cholestatic hepatitis.

**Keywords:** **Cholestasis, Intrahepatic • Gene Regulatory Networks • Hypericum • Medicine, Chinese Traditional • Pharmacology • Quercetin**

Full-text PDF: <https://www.medscimonit.com/abstract/index/idArt/928402v>

 3749  4  8  38



## Background

Cholestasis is a clinical syndrome involving liver lesions caused by abnormal bile formation, secretion, and excretion. Cholestatic liver diseases are closely associated with disorders in bile acid synthesis and transport and frequently cause cholestatic liver injury, which may ultimately progress to liver fibrosis, cirrhosis, and liver failure [1,2].

Cholestasis is one of the main causes of cholestatic hepatitis, and alpha-naphthylisothiocyanate (ANIT)-induced cholestasis and can ultimately result in cholestatic hepatitis. ANIT is a chemical toxin used to induced hepatocellular necrosis, bile duct hyperplasia, and liver fibrosis, which is used to produce a liver injury or cholestatic hepatitis in experimental animal models. In research studies, rats are intraperitoneally injected with ANIT to replicate cholestatic hepatitis [3-5]. The histopathological features of liver injury during cholestasis involve liver tissue necrosis, bile duct proliferation, hydropic changes, inflammation, and fibrosis. ANIT-induced cholestasis in animals exhibits significant elevation in plasma biomarkers of liver injury, such as alanine aminotransferase (ALT), aspartate aminotransferase (AST), alkaline phosphatase, and  $\gamma$ -glutamyltranspeptidase ( $\gamma$ -GGT). Oxidative stress is also significantly increased, as evidenced by high levels of reactive oxygen species, lipid peroxidation, depleted glutathione reservoirs, and impaired tissue antioxidant capacity in the liver. More importantly, ANIT-induced animals show an inhibition of mitochondrial dehydrogenase activity, a collapse of mitochondrial membrane potential, and mitochondrial swelling. Mitochondria from ANIT-induced cholestatic rats exhibit increased susceptibility to mitochondrial permeability transition pore opening and decreased repolarization of ATPase activity. Consequently, cholestatic hepatitis is closely associated with liver function, oxidative stress, and the structure and functions of mitochondria [6,7].

At present, only a few drugs, such as ursodeoxycholic acid (UCDA), are used in the treatment of cholestasis [8,9]; but these drugs have disadvantages, including poor response, adverse reactions, and low compliance. However, traditional Chinese medicine has a long history and rich clinical experience in treating liver diseases, such as intrahepatic cholestasis. *Hypericum japonicum* is the dried whole grass of *Hypericum japonicum* Thunb. ex Murray, also known as Di-er-cao or Tian-ji-huang, which has been used in jaundice treatment since the Qing dynasty. *H. japonicum* has the functions of clearing heat, removing dampness, calming the liver, and enhancing the gallbladder and is commonly used in the clinical treatment of damp-heat jaundice [10]. The chemical composition of *H. japonicum* includes flavonoids, xanthonoids, chromone glycosides, phloroglucinol derivatives, and lactones. Among the flavonoids, quercitrin, isoquercitrin, and quercetin-7-O- $\alpha$ -l-rhamnoside are the ingredients with hepatoprotective activity [11]. Ning Wang et al demonstrated that

the aqueous extracts of *H. japonicum*, including quercitrin, isoquercitrin, and quercetin, possess an antihepatotoxic and anticholestasis effect on carbon tetrachloride-induced hepatitis and ANIT-induced cholestasis experimental animals [12]. However, the mechanisms and targets of *H. japonicum* in the treatment of intrahepatic cholestasis are still unclear.

In this study, network pharmacology and pharmacological experiments were combined. First, the main active components and targets of *H. japonicum* were identified in silico and used to construct a component-target network [13,14]. Functional enrichment analyses of target genes were carried out to explore possible therapeutic mechanisms in the treatment of cholestatic hepatitis. Then, a rat model of cholestatic hepatitis induced by ANIT was used to reveal the mechanisms underlying the effects of *H. japonicum* in the treatment of cholestatic hepatitis and its protective effects on the liver. Specifically, we investigated mitochondrial membrane potential, hepatocyte apoptosis, regulation of intrahepatic bile acid homeostasis, and other pathways.

## Material and Methods

### Chemicals and Reagents

*H. japonicum* Thunb. ex Murray was purchased from Kangmei Pharmaceutical Co., Ltd. (Puning, China);  $\alpha$ -naphthyl isothiocyanate (ANIT, 98%) was purchased from Shanghai Macklin Biochemical Co., Ltd. (Shanghai, China); quercetin (>98.0%) and ursodeoxycholic acid (UCDA, >98%) were purchased from Dalian Melone Biology Technology Co., Ltd. (Dalian, China). Olive oil was purchased from Sigma Aldrich Trading Co., Ltd. (Shanghai, China). Malondialdehyde (MDA), superoxide dismutase (SOD), direct bilirubin (DBIL), total bilirubin (TBIL), total bile acid (TBA), ALT, and AST assay kits and glutathione peroxidase (GSH-Px) kits were purchased from the Nanjing Jiancheng Bioengineering Institute (Nanjing, China). The Bio-Rad DC protein assay reagent package was purchased from Bio-Rad Laboratories (CA, USA). HyPure molecular biology grade water, FastStart Universal SYBR Green Master mix (Rox), and RevertAid First Strand cDNA synthesis kit were purchased from Thermo Fisher Scientific Co., Ltd. (Shanghai, China). The primers against PTGS2, B-cell lymphoma-2 (BCL2), cholesterol 7-alpha hydroxylase (CYP7A1), farnesoid X receptor (FXR), interleukin-1 beta (IL-1 $\beta$ ), and tumor necrosis factor alpha (TNF- $\alpha$ ) were purchased from Servicebio Technology Co., Ltd. (Wuhan, China). All other chemicals and reagents were of analytical grade or higher and were purchased from commercial sources.

### Animals

Male Sprague-Dawley rats weighing 180 g to 220 g were purchased from the Center for Experimental Animals of Southern

Medical University (SCXK(YUE) 2018-0085). The rats were housed in cages with food and water provided ad libitum and acclimated to the laboratory for 1 week prior to each experiment. All procedures involving animals and care were approved by the Committee on the Use of Human and Animal Subjects in the Teaching and Research Department of Guangzhou University of Medicine. The animal certification number was 44002100016560.

### Screening of Components and Targets of *H. japonicum*

Taking “Di-er-cao” as the search keyword, we searched for the chemical ingredients and related targets of *H. japonicum* in the Traditional Chinese Medicine Systems Pharmacology database, which is a valuable platform for systems pharmacology research of Chinese herbal medicines and a database of network relationships between drugs, targets, and diseases [15]. The gene names corresponding to the targets were obtained using the UniPort Knowledgebase, a central hub for the collection of functional information on proteins [16]. The organism was selected as “human”.

### Therapeutic Target Prediction and Network Construction

“Cholestatic hepatitis” was used as the keyword to obtain protein targets and corresponding gene names for cholestatic hepatitis in the GeneCards database, which automatically mines and integrates human gene-centric information from myriad data sources [17]. Targets with “gifts  $\geq 30$ ” was selected as therapeutic targets for cholestatic hepatitis. To obtain the potential targets of *H. japonicum* for the treatment of cholestatic hepatitis, the drug targets and the disease targets were intersected according to the “gene name”. Cytoscape 3.7.2 software [18] was used to construct the component-target network, and the network analyzer function was used to analyze the network topology parameters.

### Target Protein Interaction Analysis

The intersection targets of *H. japonicum* and cholestatic hepatitis were imported into the String database, which can reveal direct (physical) and indirect (functional) protein-protein interactions (PPI) [19]. With high confidence (0.9) as the screening condition, removing the isolated targets, and defining the species as human, a PPI network was created. After importing the above data into Cytoscape, the Maximal Clique Centrality (MCC) analysis method in the cytoHubba plug-in was used to analyze the key regulatory targets of the PPI network.

### Target Function and Pathway Enrichment Analysis

To further understand the biological processes and signaling pathways of target protein genes, the targets for the treatment of

cholestatic hepatitis by *H. japonicum* were input into Metascape, a powerful gene annotation analysis tool [20]. The species was limited to humans, and  $P < 0.01$  was set as the significance threshold. Gene Ontology (GO) functional annotation and Kyoto Encyclopedia of Genes and Genomes (KEGG) pathway enrichment analyses were carried out, and the first 20 cluster analysis results were drawn into a bar chart for visual processing using the OmicShare tools, a free online platform for data analysis and detailed implementation process, as shown in **Figure 1**.

### Therapeutic Effects of Quercetin on ANIT-induced rat Cholestatic Hepatitis

Thirty-six male Sprague-Dawley rats were randomly divided into 6 groups (n=6 per group): Group I orally received blank vehicle for 7 days and ip injection of olive oil (2 mL/kg body weight) on day 5; Group II orally received blank vehicle for 7 days; Group III was treated orally with UCDA (50 mg/kg bodyweight) for 7 days; Group IV was treated orally with high-dose quercetin (QueH; 200 mg/kg bodyweight) for 7 days; Group V was treated orally with medium-dose quercetin (QueM; 100 mg/kg bodyweight) for 7 days; and Group VI was treated orally with low-dose quercetin (QueL, 50 mg/kg bodyweight) for 7 days. The rats in Groups II–VII, were administered ANIT-olive oil solution (100 mg/kg, ip, 2 mL/kg body weight) 2 h after administration of UCDA or quercetin on day 5. The model and control groups were treated orally with a blank solvent daily [21,22].

Forty-eight hours after the last administration of ANIT, the animals were euthanized by anesthesia via ip injection (100 mg/kg pentobarbital). Blood was collected from the abdominal aorta for biochemical evaluation. The liver was immediately removed and weighed. A large portion of the liver was snap-frozen in liquid nitrogen, and the remaining tissue was fixed in 4% paraformaldehyde, processed, and embedded in paraffin for histological examination after hematoxylin and eosin (H&E) staining. Hepatic injury was evaluated based on the levels of ALT, AST, DBIL, TBIL, TBA, and  $\gamma$ -GGT using a Chemray 240 Automatic Biochemical Analyzer (Rayto Life and Analytical Sciences Co., Ltd., Shenzhen, China). The levels of MDA, GSH-Px, and SOD were evaluated using commercial kits according to the manufacturer’s instructions, and histological assessment and scoring was conducted according to standardized criteria by a pathologist blinded to the study. For real-time reverse transcription-polymerase chain reaction (RT-PCR) analysis, liver tissue was quickly frozen in liquid nitrogen and stored at  $-80^{\circ}\text{C}$  until analysis.

### Analysis of PTGS2, BCL2, CYP7A1, FXR, IL-1 $\beta$ , and TNF- $\alpha$ mRNAs by RT-PCR

Total RNA was extracted from liver tissues using TRIzol, according to the manufacturer’s instructions (Servicebio, Wuhan, China).

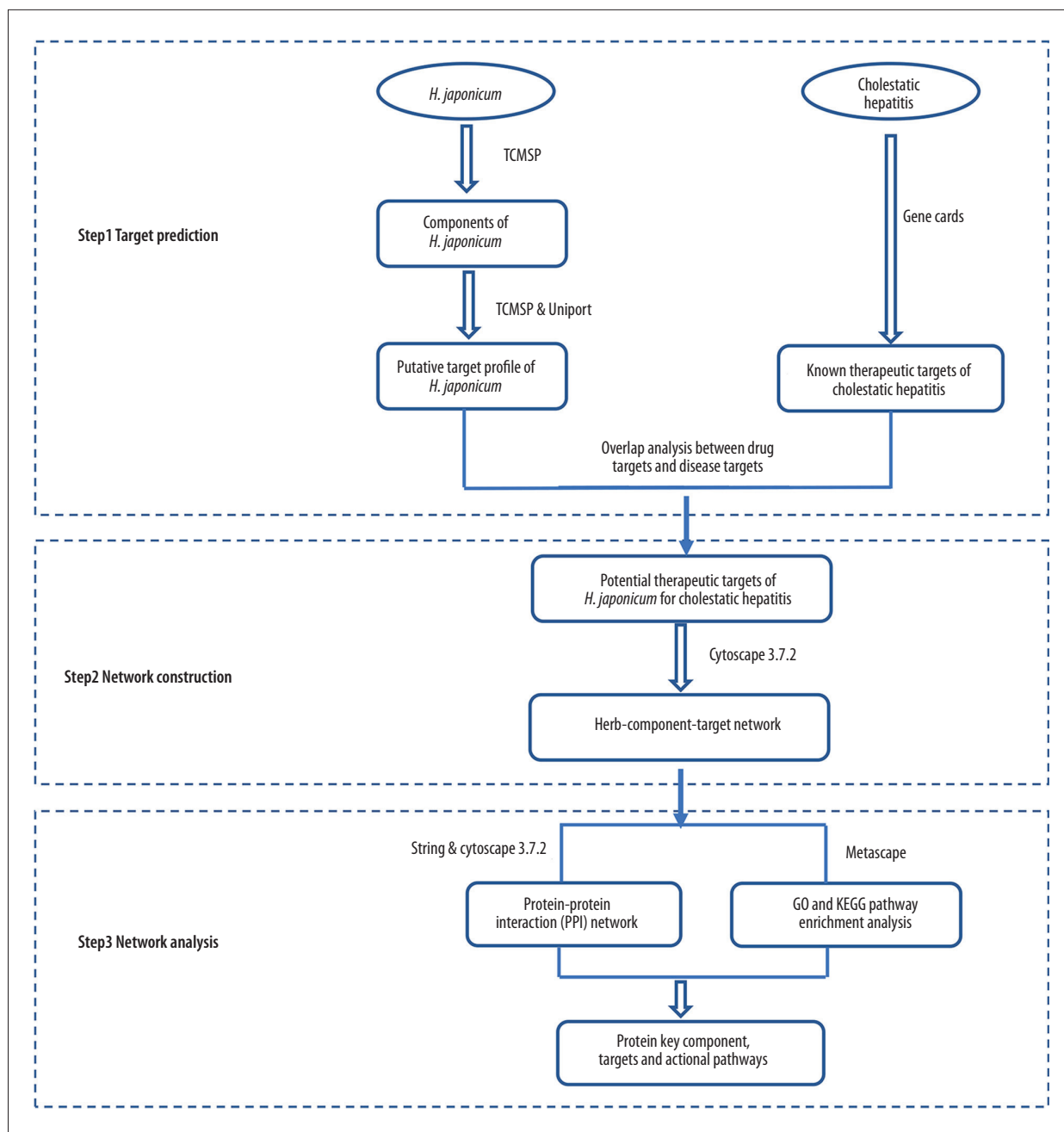


**Figure 1.** The detailed implementation process of the network pharmacology research.

Total RNA (10  $\mu$ L) was reverse-transcribed into cDNA. PCR reactions (20  $\mu$ L) for GAPDH, PTGS2, BCL2, CYP7A1, FXR, TNF- $\alpha$ , and IL-1 $\beta$  contained 2  $\mu$ L cDNA, 2  $\mu$ L 2.5  $\mu$ M primer, 10  $\mu$ L qPCR mix, and 6  $\mu$ L ddH<sub>2</sub>O. The reactions were incubated at 65°C for 10 min, then at 42°C for 60 min, and terminated at 72°C for 15 min. The PCR primer sequences are listed in **Table 1**. RT-PCR reactions were performed as follows: a pre-cycling stage at 95°C for 10 min, followed by 40 cycles of denaturization at 95°C for 30 s, and annealing at 60°C for 60 s. The melting curve was from 65°C to 95°C with a ramp rate of 0.3°C/15 s. Fluorescence

was measured at the end of each annealing step, and the melting curves were monitored to confirm the specificity of the PCR products. The  $2^{-\Delta\Delta CT}$  method was used to determine the mRNA expression levels of PTGS2, BCL2, CYP7A1, FXR, IL-1 $\beta$ , and TNF- $\alpha$  mRNAs relative to the control gene GAPDH.

### Statistical Analysis

All data were expressed as mean  $\pm$  standard deviation (SD). Statistical analysis was performed using GraphPad Prism 8.

**Table 1.** Primers for real-time reverse transcription-polymerase chain reaction (RT-PCR).

Gene	Primer sequences (5'-3')
GAPDH	CCTCGTCCCCTAGACAAAATG
	TGAGGTCAATGAAGGGTTCGT
PTGS2	CTGATGACTGCCCAACTCCC
	CTGGGCAAAGAATGCGAACA
BCL2	TTGTGGCCTTCTTGAGTTCTG
	GCATCCCAGCCTCCGTTAT
FXR	TGCCTGTGACAAAGAAGCCG
	CATTGAGCAACATTCCCATC
CYP7A1	GGCATCTCAAGCAAACACCAT
	GCTGTGCGGATATTCAAGGAT
IL-1 $\beta$	TCAAATCTCGCAGCAGCACATC
	CGTCACACACCAGCAGTTATC
TNF- $\alpha$	CCCTCACACTCACAACCACC
	CTTGAGATCCATGCCGTTG

3.0 (GraphPad Software Inc., San Diego, CA, USA). The data were analyzed by one-way analysis of variance (ANOVA), followed by the Dunnett's test.  $P < 0.05$  was considered statistically significant.

## Results

### Components and Targets of *H. japonicum*

To fully investigate the components of *H. japonicum*, we did not set the pharmacokinetic parameters, such as oral bioavailability and drug-likeness as screening criteria. Through the TCMSP database, 49 active components and 499 corresponding targets of *H. japonicum* were obtained. After removing duplicates and correcting names by Uniprot, 269 targets were retained. The active components of *H. japonicum* and the parameter information are shown in **Table 2**.

**Table 2.** The active components of *Hypericum japonicum*.

MOL ID	Molecule name	MW	OB%	DL
MOL000069	Palmitic acid	256.48	19.3	0.1
MOL000098	Quercetin	302.25	46.43	0.28
MOL000105	Protocatechuic acid	154.13	25.37	0.04
MOL000114	Vanillic acid	168.16	35.47	0.04
MOL000166	ZINC01609418	222.41	21.62	0.07
MOL000193	(Z)-caryophyllene	204.39	30.29	0.09
MOL000211	Mairin	456.78	55.38	0.78
MOL000358	beta-sitosterol	414.79	36.91	0.75
MOL000359	Sitosterol	414.79	36.91	0.75
MOL000414	Caffeate	180.17	54.97	0.05
MOL000422	Kaempferol	286.25	41.88	0.24
MOL000437	Hirsutrin	464.41	1.86	0.77
MOL000676	DBP	278.38	64.54	0.13
MOL000701	Quercitrin	448.41	4.04	0.74
MOL000861	Healip	326.68	11.65	0.22
MOL001955	Heriguard	354.34	11.93	0.33
MOL002067	Hypericin	504.46	14.66	0.08
MOL002378	UND	156.35	17.15	0.02
MOL002622	Filicin	668.8	6.71	0.63



**Table 2 continued.** The active components of *Hypericum japonicum*.

MOL ID	Molecule name	MW	OB%	DL
MOL003228	Norathyriol	260.21	18.35	0.22
MOL004459	Tridecanol	200.41	15.18	0.04
MOL004746	(E,7S,11R)-3,7,11,15-tetramethylhexadec-2-en-1-ol	296.6	33.82	0.13
MOL004783	Nonane	128.29	29.23	0.01
MOL005810	Lauryl palmitate	424.84	14.45	0.43
MOL006771	Poriferasterol monoglucoside	574.93	21.32	0.63
MOL006772	Poriferasterol monoglucoside_qt	412.77	43.83	0.76
MOL007860	Quercetin-7-rhamnoside	448.41	15.5	0.76
MOL007861	Sarothralin	534.65	4.24	0.72
MOL007862	Uliginosin B	498.62	28.1	0.73
MOL007863	Saroaspidin A	446.54	5.74	0.48
MOL007864	Saroaspidin B	460.57	21.45	0.52
MOL007865	Saroaspidin C	474.6	5.57	0.55
MOL007866	Japonicin A	460.57	15.8	0.5
MOL007867	Japonicine B	566.75	3.92	0.78
MOL007868	Japonicine C	534.65	4.22	0.72
MOL007869	Japonicine D	668.8	1.6	0.64
MOL007870	Sarothralen A	568.77	0.97	0.69
MOL007871	Sarothralin G	602.78	0.96	0.7
MOL007872	Quercetin-7-O-rhamnoside	448.41	2.6	0.76
MOL007873	Isoamyl laurate	270.51	23.92	0.11
MOL007874	Lauryl stearate	452.9	13.92	0.46
MOL007875	Mesylmethane	94.15	40.12	0.00
MOL007876	2,4-dimethylheptane	128.29	35.9	0.01
MOL007877	n-Tetra-triacontanoic acid	530.69	10.54	0.5
MOL007878	4H-1-Benzopyran-4-one, 2-(3,4-dihydroxyphenyl)-3-(alpha-D-galactopyranosyloxy)-5,7-dihydroxy-	464.41	2.41	0.77
MOL007879	Tetramethoxyluteolin	342.34	43.68	0.37
MOL007880	3,5,7,3',5' pentahydroxy flavonol	290.29	63.64	0.24
MOL007881	1,3,5,6-tetrahydroxyxanthone	260.21	16.22	0.22
MOL007882	Xanthone der.	244.21	18.16	0.19

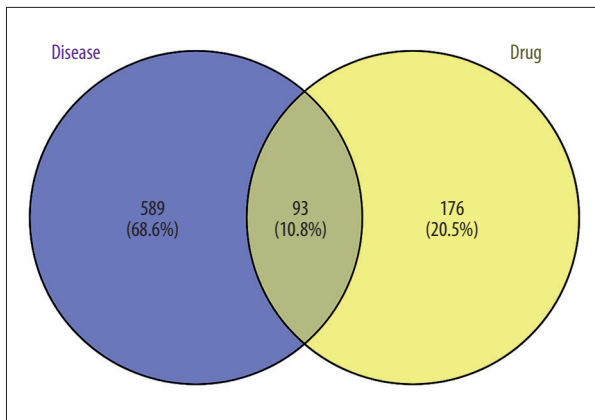


**Figure 2.** Venn diagram of the targets of *Hypericum japonicum* and cholestatic hepatitis.

### Targets of *H. japonicum* in the Treatment of Cholestatic Hepatitis

In the GeneCards database, 682 targets of cholestatic hepatitis were screened. Finally, 93 targets that may be related to the *H. japonicum* treatment of cholestatic hepatitis were obtained by crossing the targets of active components and disease (Figure 2).

### Compound-target Network

The component-target network of *H. japonicum* in the treatment of cholestatic hepatitis consisted of 115 nodes and 175 edges, with 22 hexagonal nodes representing active components and 93 V-shaped nodes representing targets (Figure 3).

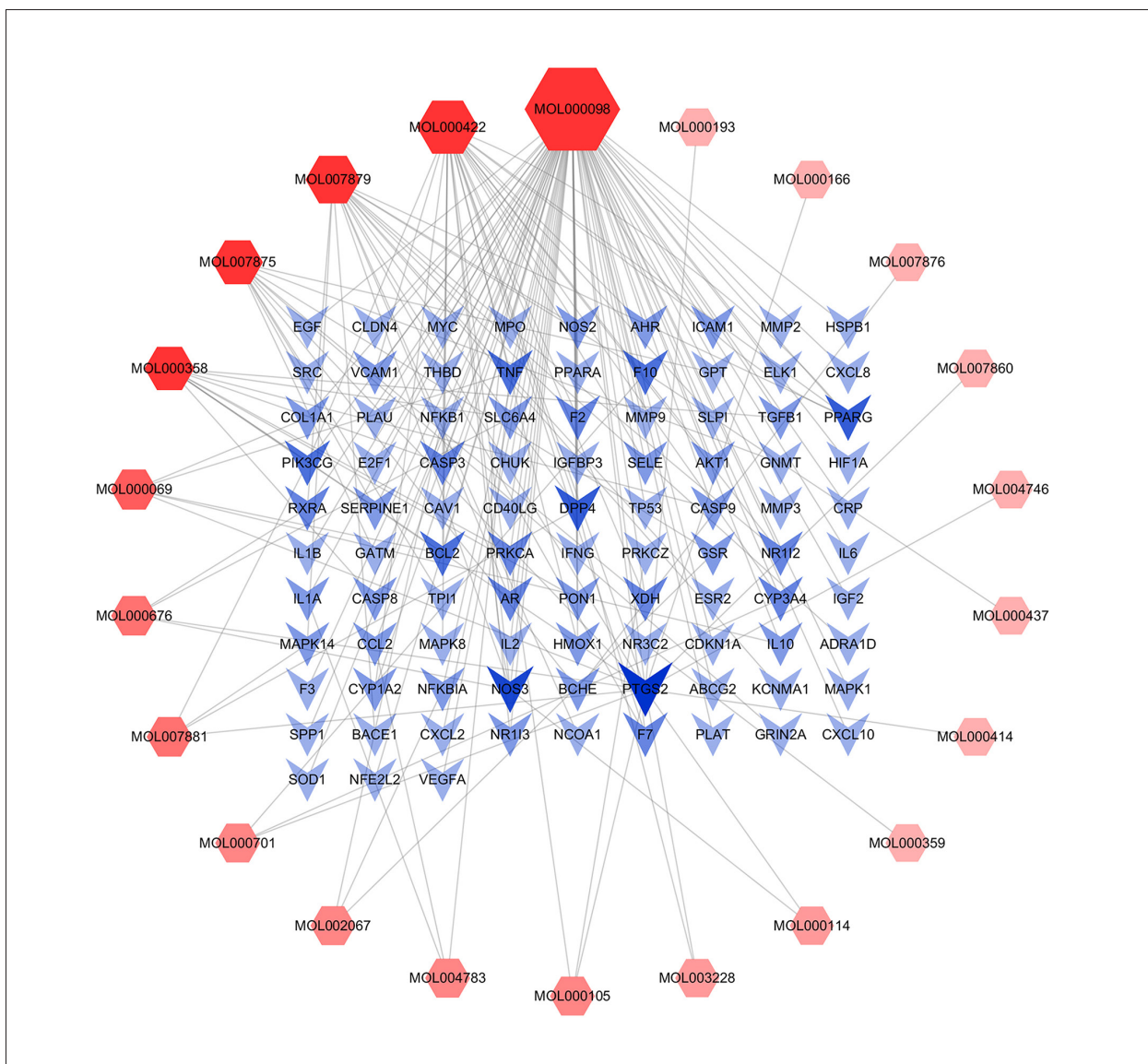


**Figure 3.** The compound-target network of *Hypericum japonicum* in the treatment of cholestatic hepatitis.

**Table 3.** The node characteristic parameters of the main active ingredients in compound-target network.

MOL ID	Component name	Degree	Betweenness	Closeness
MOL000098	Quercetin	74	0.756382	0.643678
MOL000422	Kaempferol	26	0.100813	0.408759
MOL007879	Tetramethoxyluteolin	17	0.117672	0.386207

**Table 4.** The node characteristic parameters of the main targets in the compound-target network.

Target	Target name	Degree	Betweenness	Closeness
PTGS2	Prostaglandin G/H synthase 2	17	0.240087	0.525822
NOS3	Nitric oxide synthase, endothelial	6	0.021565	0.435798
PPARG	Peroxisome proliferator activated receptor gamma	5	0.009116	0.425856
DPP4	Dipeptidyl peptidase IV	5	0.020751	0.432432
BCL2	Apoptosis regulator Bcl-2	4	0.006814	0.413284
TNF	Tumor necrosis factor	4	0.011948	0.410256
PIK3CG	Phosphatidylinositol-4,5-bisphosphate 3-kinase catalytic subunit, gamma isoform	4	0.008965	0.416357
F10	Coagulation factor X	4	0.028392	0.422642

The size and transparency of the nodes were set according to degree. The higher the degree value, the larger the node, and the darker the color, the greater the connectivity and importance. As shown in the results, *H. japonicum* had multi-component and multi-target action; that is, 1 compound interacting with multiple targets, and different compounds interacting with the same target. According to the network topology parameters, such as degree, betweenness, and closeness, the main active components were quercetin, kaempferol, and tetramethoxyluteolin (Table 3), and the core targets were PTGS2, nitric oxide synthase (NOS3), peroxisome proliferative activated receptor gamma (PPARG), dipeptidyl peptidase IV (DPP4), BCL2, and TNF (Table 4).

### PPI Network

The interaction of 93 drug-disease intersection targets was analyzed using the STRING database. High confidence (0.9) was set, isolated targets were hidden, and a PPI network with 81 targets and 299 interaction links was obtained (Figure 4A). Applying the MCC algorithm of cytoHubba, the top 10 core regulatory targets in the PPI network were TNF, IL6, IL1B, CXCL8, IL10, CCL2, ICAM1, NFKB1, NFKBIA, and MYC (Figure 4B).

### Target Function and Pathway Enrichment

The GO functional annotation and KEGG pathway enrichment analyses of therapeutic targets were carried out using

Metascape. A total of 1899 GO items were obtained, including 41 items for cell composition, 105 items for molecular function, and 1753 items for biological process. The main biological processes and cellular component in which *H. japonicum* was involved included responses to lipopolysaccharide, cytokine-mediated signaling, apoptotic signaling, membrane raft (Figure 5A, 5B), and molecular functions including cytokine receptor binding, transcription factor binding, and serine-type endopeptidase activity (Figure 5C). In total, 146 KEGG signaling pathways were analyzed, with the most notable being the AGE-RAGE and TNF signaling pathways and hepatitis B, arginine biosynthesis, and bile secretion. (Figure 5D).

### Quercetin Protected Against ANIT-induced Cholestatic Hepatitis in Rats

In the intrahepatic cholestasis rat model, quercetin restored the liver/body weight ratio in liver injury with cholestasis (Figure 6). The serum ALT, AST, DBIL, TBIL, TBA, and  $\gamma$ -GGT, which were used to evaluate intrahepatic bile duct proliferation and cholestasis associated with hepatic cell damage, were drastically increased in the model rats. In contrast, quercetin dose-dependently reduced serum ALT, AST, DBIL, TBIL, TBA, and  $\gamma$ -GGT levels. Similarly, quercetin treatment ameliorated ANIT-induced hepatic oxidative stress, increased serum SOD and GSH-Px levels, and decreased MDA levels (Figure 7).



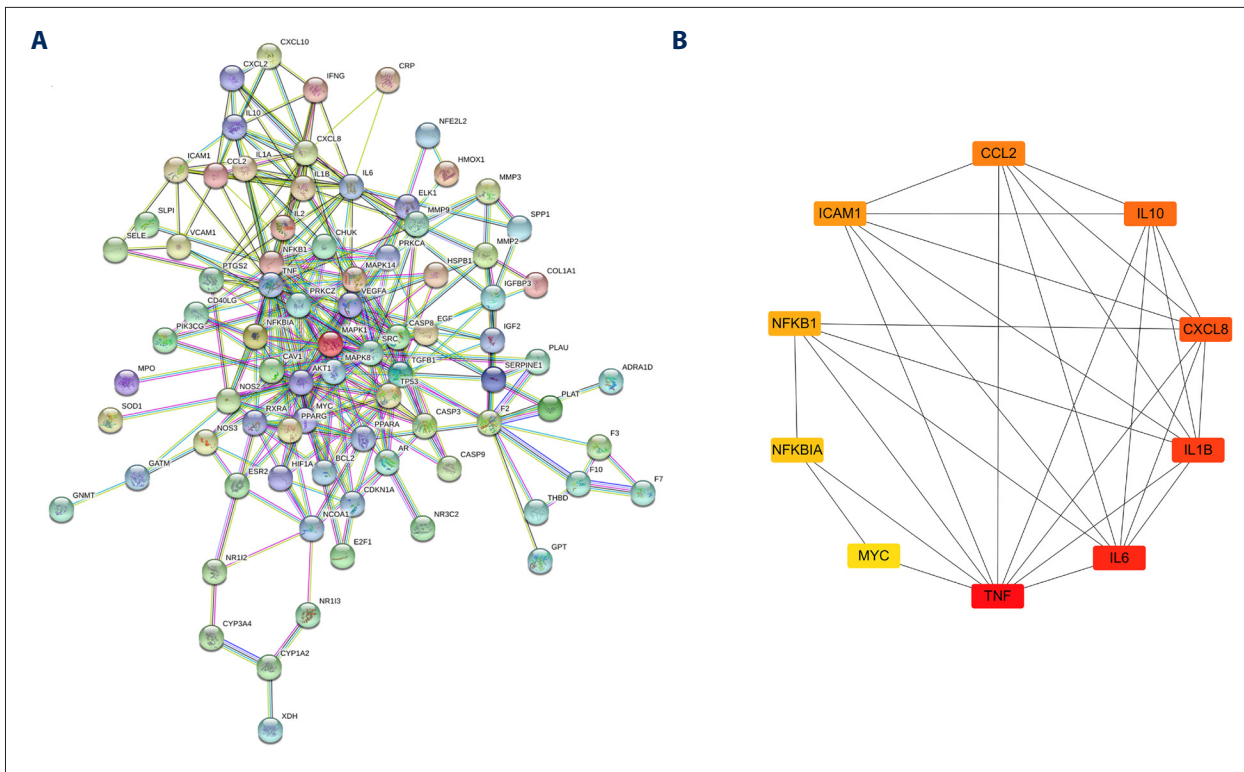


**Figure 4.** The network and key subnetwork of protein-protein interaction (PPI) of potential targets. (A) PPI network; (B) key subnetwork for PPI.

Histological evaluations by H&E staining provided direct proof of the preventive and therapeutic effects of quercetin on ANIT-induced intrahepatic cholestasis. H&E staining showed that the liver tissue of the control group exhibited a normal microstructure, the hepatic lobules were clear, and the liver cell cable was neat and orderly, without abnormal morphological changes. In contrast, ANIT-treated liver sections showed indistinct liver lobule structure, hepatic cord derangement, hepatic swelling, hyperemia, and necrosis (Figure 8A). However, quercetin significantly attenuated the degree of hepatic putrescence and inflammatory cell infiltration, displaying a dose-effect relationship. These results revealed that quercetin protected against ANIT-induced liver injury originating from intrahepatic cholestasis in rats.

#### Quercetin Protected PTGS2, BCL2, CYP7A1, FXR, IL-1 $\beta$ , and TNF- $\alpha$ mRNA Expression

To further evaluate the protective effect of quercetin on hepatocytes in ANIT-induced intrahepatic cholestatic liver injury rats, the mRNA levels of PTGS2, BCL2, CYP7A1, FXR, IL-1 $\beta$ , and TNF- $\alpha$  were measured using RT-PCR. As shown in Figure 8B, compared with that of control mice, PTGS2, CYP7A1, IL-1 $\beta$ , and TNF- $\alpha$  were upregulated in the ANIT model group, but BCL2 and FXR were downregulated. However, administration of quercetin (at doses of 50, 100, and 200 mg/kg) and UCDA

significantly decreased the expression of PTGS2, CYP7A1, IL-1 $\beta$ , and TNF- $\alpha$  mRNA by 44.4% ( $P < 0.05$ ), 60.3% ( $P < 0.01$ ), 49.2% ( $P < 0.05$ ), and 34.1% ( $P < 0.05$ ), respectively, and increased the expression of BCL2 and FXR mRNA by 92.9% and 167.6% ( $P < 0.01$ ), respectively, vs the ANIT model group. These results showed that quercetin could protect hepatocytes by accelerating the excretion and transport of bile acids, maintaining the mitochondrial membrane potential of hepatocytes, and inhibiting inflammation.

#### Discussion

Collectively, we used an ANIT-induced rat model, which showed *H. japonicum* can be a treatment of cholestatic hepatitis. Network pharmacology and pharmacodynamics experiments elucidated the effect and molecular mechanism of *H. japonicum* in the treatment of cholestatic hepatitis and provided a theoretical basis for further research and clinical application of the herb.

The main chemical constituents of *H. japonicum* are flavonoids [23], phloroglucinol derivatives, and dipeptides, among others [11]. Puthur et al determined that the IC<sub>50</sub> of *H. japonicum* acetonic extracts on ascites cells is 29.30  $\mu\text{g}/\text{mL}$ , with their results showing a good anti-tumor activity in vitro and

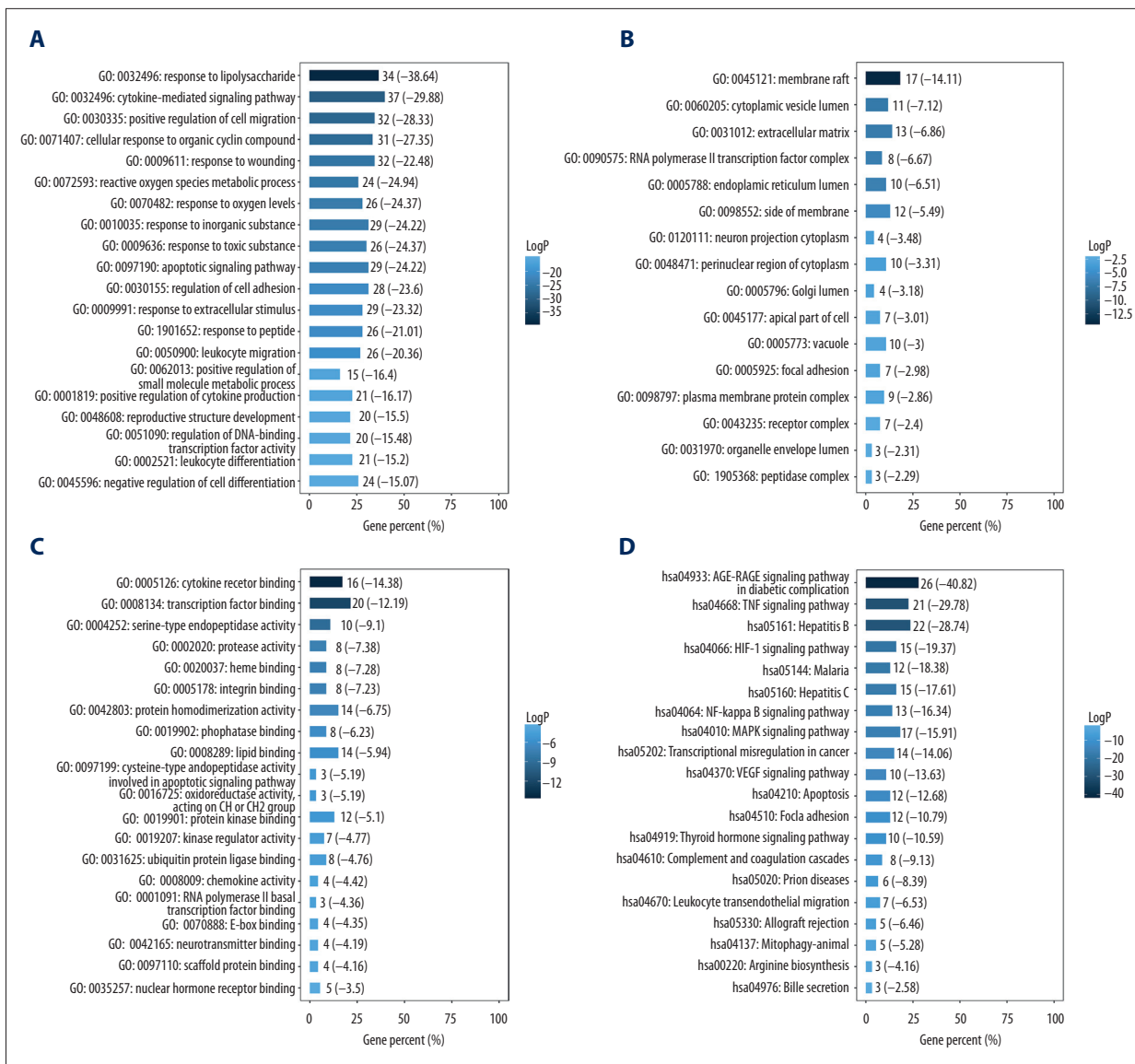


**Figure 5.** Enrichment analyses of potential targets of *Hypericum japonicum* in the treatment of cholestatic hepatitis (A) Gene Ontology-biological process analysis; (B) Gene Ontology-cell composition analysis; (C) Gene Ontology-molecular function analysis; (D) Encyclopedia of Genes and Genomes analysis.

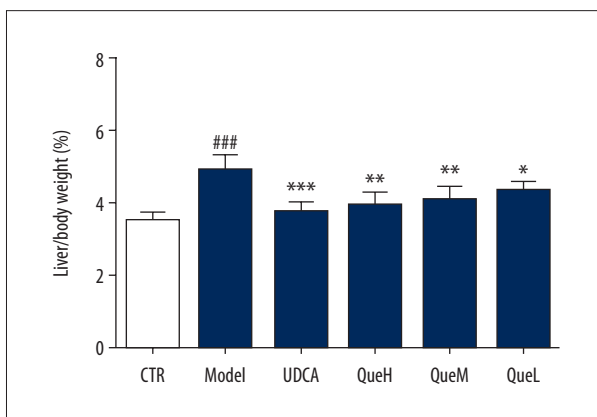


**Figure 6.** Effect of quercetin treatment on the liver/body weight ratio. #P <0.05, ## P<0.01, ### P<0.001 vs control group; \* P<0.05, \*\* P<0.01, \*\*\* P<0.001 vs model group. Data represent mean±SD (n=6 for each group). Groups were as follows: ursodeoxycholic acid (UDCA), control (CTR), high-dose quercetin (QueH; 200 mg/kg bodyweight), medium-dose quercetin (QueM; 100 mg/kg bodyweight), low-dose quercetin (QueL, 50 mg/kg bodyweight).

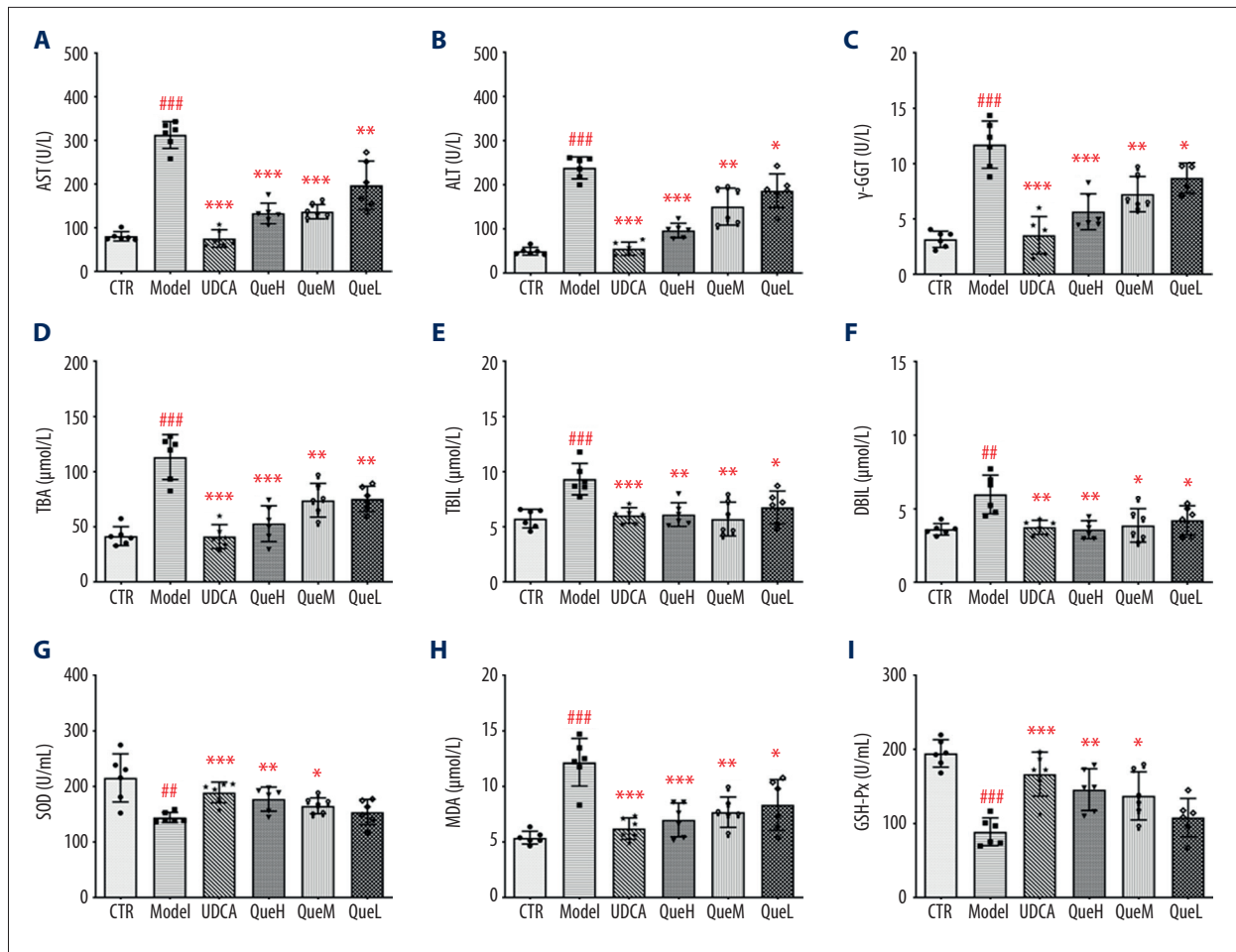


**Figure 7.** Effect of quercetin treatment on the levels of serum biochemical indices in ANIT administration rats. (A) aspartate aminotransferase (AST); (B) alanine aminotransferase (ALT); (C)  $\gamma$ -glutamyltranspeptidase ( $\gamma$ -GGT); (D) total bile acid (TBA); (E) total bilirubin (TBIL); (F) direct bilirubin (DBIL); (G) superoxide dismutase (SOD); (H) malondialdehyde (MDA); and (I) glutathione peroxidase (GSH-Px). #  $P < 0.05$ , ##  $P < 0.01$ , ###  $P < 0.001$  vs control group; \*  $P < 0.05$ , \*\*  $P < 0.01$ , \*\*\*  $P < 0.001$  vs model group. Data represent mean  $\pm$  SD (n=6 for each group).

that the methanolic extracts of *H. japonicum* has a synergistic effect on pests by inhibition of some key enzymes. Their experiments revealed that *H. japonicum* has various biological activities that requires further investigation [24,25]. Modern pharmacological studies have shown that the extract of *H. japonicum* has a variety of biological activities, including hepatoprotective, antioxidative, anti-inflammatory, and antitumor effects. *H. japonicum* and its main components protect against carbon tetrachloride-induced hepatitis, ANIT-induced cholestasis, and anti-duck hepatitis A viral activity and improve liver function and oxidative damage [12,26]. Isoquercitrin and quercetin 7-rhamnoside are the main active hepatoprotective ingredients [11,27]. The present study showed that quercetin, the principal constituent of *H. japonicum*, can reduce ANIT-induced hepatocyte degeneration and necrosis, and reduce the degree of liver injury. H&E results further confirmed the protective effect of quercetin on cholestatic hepatitis.

In the present study, we combined network pharmacology research with animal pharmacological experiments. First, we screened the main active components and targets of *H. japonicum* in the treatment of cholestatic hepatitis. We then constructed a “component-target” network and analyzed the functional enrichment of the targets to explore the possible mechanism of its therapeutic action against cholestatic hepatitis. Finally, we verified those targets and molecular mechanisms through animal experiments. The biochemical indexes and pathological characteristics of intrahepatic cholestasis that we observed were consistent with human diseases, supporting the clinical relevance of our rat model of cholestatic hepatitis.

The serum level of bile acid is considered crucial evidence for the clinical diagnosis of intrahepatic cholestasis disorders and their resulting liver injury. Intrahepatic cholestasis leads to the obstruction of normal excretion of bile and liver function

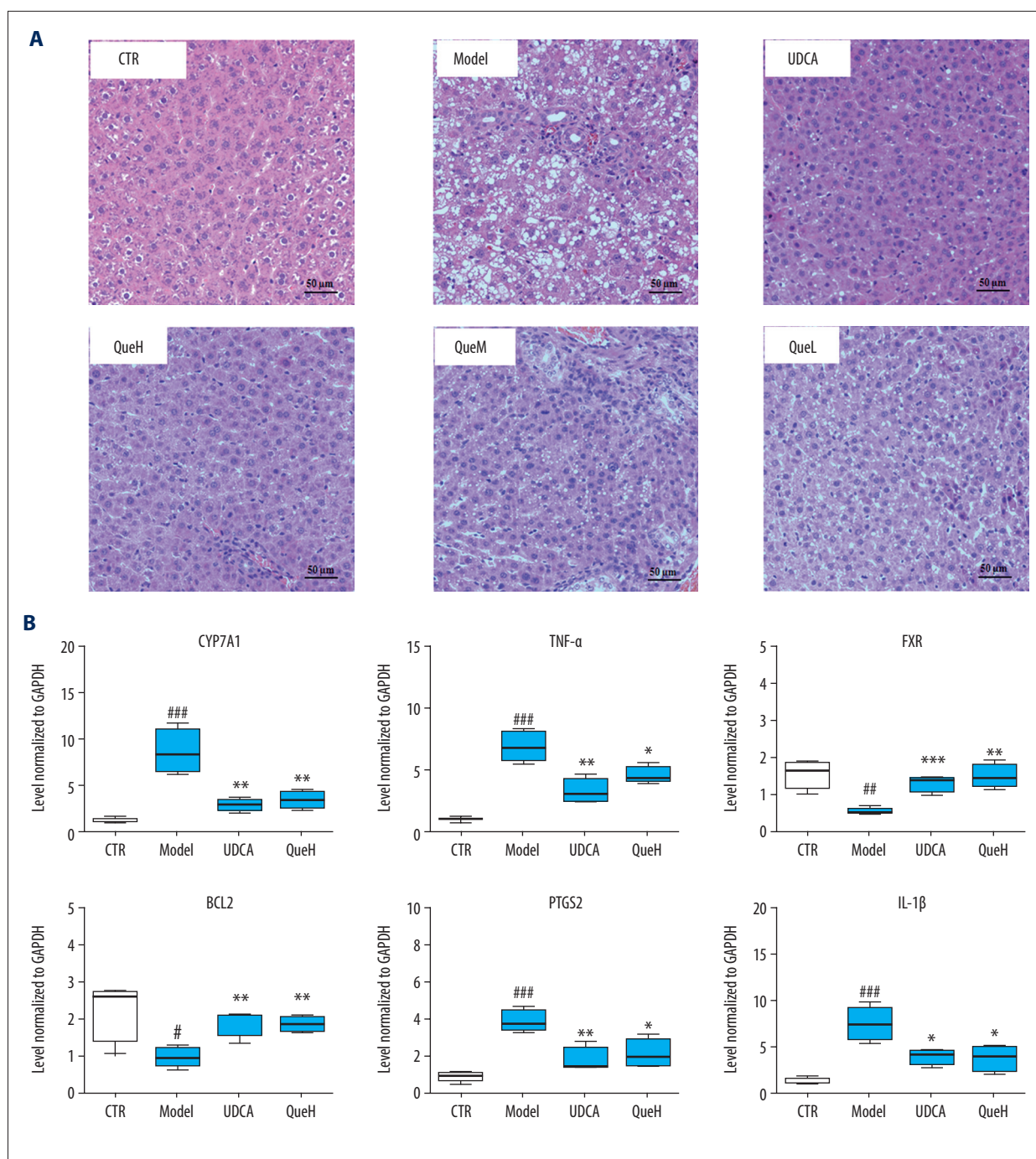


**Figure 8.** Pharmacological action and mechanisms of quercetin in alpha-naphthylisothiocyanate (ANIT)-administered rats. **(A)** Photomicrograph of the histology of the rat liver, control group shows normal liver histology. The liver histology of the untreated ANIT rat model group shows lipid vacuoles in the hepatocytes, mild inflammation, and cholestasis. The liver changes are reduced following treatment with ursodeoxycholic acid (UDCA) for 7 days; Group IV, high-dose quercetin (QueH) was treated with 200 mg/kg quercetin for 7 days; Group V, medium-dose quercetin (QueM) was treated with 100 mg/kg quercetin for 7 days; Group VI, low-dose quercetin (QueL) was treated with 50 mg/kg quercetin for 7 days. Hematoxylin and eosin (H&E) staining. Magnification  $\times 40$ ; **(B)** Restoration of PTGS2, BCL2, CYP7A1, FXR, IL-1 $\beta$ , and TNF- $\alpha$  mRNA expression in cholestatic hepatitis livers. #  $P < 0.05$ , ##  $P < 0.01$ , ###  $P < 0.001$  vs control group; \*  $P < 0.05$ , \*\*  $P < 0.01$ , \*\*\*  $P < 0.001$  vs model group. Data represent mean  $\pm$  SD ( $n = 6$  for each group).



enzymes, resulting in an increase in serum TBIL, DBIL, and TBA, and we showed that quercetin reversed ANIT-induced bile acid dysregulation. In addition, quercetin significantly reduced the serum levels of AST, ALT, and  $\gamma$ -GGT, which were dramatically increased due to the degeneration and necrosis of hepatocytes and hepatocyte membrane damage.

Lipid peroxidation is one of the important pathological mechanisms of ANIT-induced cholestatic hepatitis, causing liver cell damage [28-30]. The level of oxidative stress in the body reflects the severity of cholestatic hepatitis, which is why GSH-Px, SOD, and MDA, used to assess lipid peroxide levels, are important indicators. In the present study, each quercetin dosing group showed significantly reduced MDA, with increased SOD and GSH-Px activities. These results indicated that relief of liver cell damage by quercetin was associated with free radical scavenging, inhibition of lipid peroxidation, and reduction of the production of lipid peroxides.

Network pharmacology results indicated that the main relevant targets for the treatment of cholestatic hepatitis by *H. japonicum* include PTGS2, NOS3, PPARG, DPP4, BCL2, and TNF. In the present study, 5 targets, PTGS2, BCL2, TNF- $\alpha$ , FXR, and CYP7A1, which are associated with cholestatic hepatitis, liver fibrosis, and liver damage, were selected for molecular-level research. PTGS2, also known as cyclooxygenase 2, is a downstream molecule of the NF- $\kappa$ B pathway [31,32]. PTGS2 participates in the occurrence of inflammation by promoting cell proliferation, inhibiting cell apoptosis, promoting angiogenesis, and inhibiting immune function. TNF- $\alpha$  is an important inflammatory mediator that participates in the process of cholestasis. In our study, the expression levels of PTGS2, TNF- $\alpha$  protein, and mRNA were up-regulated in the liver tissues of the ANIT-induced cholestatic liver injury model rats, suggesting that PTGS2 overexpression may promote acute liver injury and the development of cholestasis.

BCL2 is a protein that inhibits cell apoptosis. It prevents oxidative damage and DNA fragmentation of cell components and regulates anti-oxidative pathways [33]. It also improves mitochondrial membrane potential and inhibits mitochondrial release of cytochrome C and apoptosis-inducing factor by affecting cell membrane transport, thereby inhibiting liver cell apoptosis and other effects [34,35].

FXR is a bile acid receptor that regulates the homeostasis of bile acid in the liver [36]. It inhibits the activity of the bile acid synthesis rate-limiting enzyme CYP7A1 through negative feedback regulation mediated by a small heterodimer chaperon and reduces the synthesis of bile acid. At the same time, FXR can upregulate the expression of the transporters BSEP and MRP2 on the side membrane of the hepatocyte bile duct, accelerating the excretion and transport of bile acids in order to protect liver cells [37,38].

Our results showed that model rats have a large amount of cholic acid stasis under the action of ANIT, leading to down-regulation of FXR expression and a consequent increase of CYP7A1 expression. Also, the downregulated expression of FXR caused a decrease in the expression of the downstream genes BSEP and MRP2, which it regulates. Quercetin intervention significantly restored the expression level of FXR in rat liver tissues and regulated the expression of its downstream genes CYP7A1, BSEP, and MRP2 in the opposite direction of the model group. The results of this study are in agreement with previous research conclusions.

ANIT-induced cholestatic hepatitis has biochemical and pathological changes that are similar to those of humans. However, the pathological process of the single ANIT treatment was short in the present study, restricting the research that normally requires a longer experimental period of 48 to 72 h. Multiple intermittent administration of ANIT will overcome this disadvantage. Network pharmacology of traditional Chinese medicine takes the chemical compositions found in medicinal materials as the research object; however, the chemical substances involved in the drug efficacy of traditional Chinese medicine are not necessarily a single component because the effective substance may be a group of pharmacodynamic components. Because the targets and pathways of substances in traditional Chinese medicine are usually known, there are limitations for discovery of new mechanisms. In the future, artificial intelligence algorithms can be combined with network pharmacology to obtain more comprehensive and objective information.

## Conclusions

In summary, with the help of active ingredients such as quercetin, *H. japonicum* can activate FXR, inhibit CYP7A1, reduce the synthesis of bile acid in hepatocytes, and increase the extrahepatic excretion of bile acid. Also, it can regulate BCL2 to improve mitochondrial membrane potential, inhibit hepatocyte apoptosis, and regulate the homeostasis of bile acid in the liver. Further, by inhibiting the expression of PTGS2, IL-1 $\beta$ , and TNF- $\alpha$ , it can interfere with the inflammatory response. In brief, according to the network pharmacology analysis, quercetin, kaempferol, and tetramethoxyluteolin are the main active ingredients of *H. japonicum* for ameliorating cholestatic hepatitis. Results of this study may provide support for future research on the role of quercetin, kaempferol, and tetramethoxyluteolin in human liver disease and the roles of the PTGS2, BCL2, CYP7A1, and FXR genes in cholestatic hepatitis.

## Conflict of Interest

None.



## References:

- Wagner M, Fickert P. Drug therapies for chronic cholestatic liver diseases. *Annu Rev Pharmacol Toxicol*, 2020;60:503-27
- Kwo PY, Cohen SM, Lim JK. ACG Clinical guideline: Evaluation of abnormal liver chemistries. *Am J Gastroenterol*, 2017;112:18-35
- Dai M, Yang J, Xie M, et al. Inhibition of JNK signalling mediates PPAR $\alpha$ -dependent protection against intrahepatic cholestasis by fenofibrate. *Br J Pharmacol*, 2017;174:3000-17
- Ding Y, Zhao L, Mei H, et al. Exploration of Emodin to treat alpha-naphthylisothiocyanate-induced cholestatic hepatitis via anti-inflammatory pathway. *Eur J Pharmacol*, 2008;590:377-86
- Joshi N, Ray JL, Kopec AK, Luyendyk JP. Dose-dependent effects of alpha-naphthylisothiocyanate disconnect biliary fibrosis from hepatocellular necrosis. *J Biochem Molec Toxicol*, 2016;31(1):1-7
- Rolo A. Histological changes and impairment of liver mitochondrial bioenergetics after long-term treatment with alpha-naphthylisothiocyanate (ANIT). *Toxicology*, 2003;190:185-96
- Gomez-Quiroz LE, Seo D, Lee YH, et al. Loss of c-Met signaling sensitizes hepatocytes to lipotoxicity and induces cholestatic liver damage by aggravating oxidative stress. *Toxicology*, 2016;361-62:39-48
- Gulamhusein AF, Hirschfield GM. Primary biliary cholangitis: Pathogenesis and therapeutic opportunities. *Nat Rev Gastroenterol Hepatol*, 2020;17:93-110
- Chen HL, Wu SH, Hsu SH, et al. Jaundice revisited: Recent advances in the diagnosis and treatment of inherited cholestatic liver diseases. *J Biomed Sci*, 2018;25:75
- Wu R, Le Z, Wang Z, et al. Hyperjaponol H, a new bioactive filicinic acid-based meroterpenoid from *Hypericum japonicum* Thunb. ex Murray. *Molecules*, 2018;23:683
- Liu LS, Liu MH, He JY. *Hypericum japonicum* Thunb. ex Murray: Phytochemistry, pharmacology, quality control and pharmacokinetics of an important herbal medicine. *Molecules*, 2014;19:10733-54
- Wang N, Li P, Wang Y, et al. Hepatoprotective effect of *Hypericum japonicum* extract and its fractions. *J Ethnopharmacol*, 2008;116:1-6
- Liu TH, Chen WH, Chen XD, et al. Network pharmacology identifies the mechanisms of action of taohongsiwu decoction against essential hypertension. *Med Sci Monit*, 2020;26:e920682
- Zeng Q, Li L, Siu W, et al. A combined molecular biology and network pharmacology approach to investigate the multi-target mechanisms of Chaihu Shugan San on Alzheimer's disease. *Biomed Pharmacother*, 2019;120:109370
- Ru J, Li P, Wang J, et al. TC MSP: A database of systems pharmacology for drug discovery from herbal medicines. *J Cheminform*, 2014;6:13
- The UniProt Consortium. UniProt: The universal protein knowledgebase. *Nucleic Acids Res*, 2018;46:2699
- Stelzer G, Rosen N, Plaschkes I, et al. The GeneCards suite: From gene data mining to disease genome sequence analyses. *Curr Protoc Bioinformatics*, 2016;54:1.30.1-33
- Su G, Morris JH, Demchak B, Bader GD. Biological network exploration with Cytoscape 3. *Curr Protoc Bioinformatics*, 2014;47:8.13.1-24
- Szklarczyk D, Gable AL, Lyon D, et al. STRING v11: Protein-protein association networks with increased coverage, supporting functional discovery in genome-wide experimental datasets. *Nucleic Acids Res*, 2019;47:D607-13
- Zhou Y, Zhou B, Pache L, et al. Metascape provides a biologist-oriented resource for the analysis of systems-level datasets. *Nat Commun*, 2019;10:1523
- Yan JY, Ai G, Zhang XJ, et al. Investigations of the total flavonoids extracted from flowers of *Abelmoschus manihot* (L.) Medic against alpha-naphthylisothiocyanate-induced cholestatic liver injury in rats. *J Ethnopharmacol*, 2015;172:202-13
- Huan L, Zhou C, Hou Y, et al. Paracrine fibroblast growth factor 1 functions as potent therapeutic agent for intrahepatic cholestasis by downregulating synthesis of bile acid. *Front Pharmacol*, 2019;10:1515
- Su J, Fu P, Shen Y, et al. Simultaneous analysis of flavonoids from *Hypericum japonicum* Thunb. ex Murray (hypericaceae) by HPLC-DAD-ESI/MS. *J Pharm Biomed Anal*, 2008;46:342-48
- Puthur S, Anoopkumar AN, Rebello S, Aneesh EM. *Hypericum japonicum*: A double-headed sword to combat vector control and cancer. *Appl Biochem Biotechnol*, 2018;186:1-11
- Puthur S, Anoopkumar AN, Rebello S, Aneesh EM. Synergistic control of storage pest rice weevil using *Hypericum japonicum* and deltamethrin combinations: A key to combat pesticide resistance. *Environmental Sustainability*, 2019;2:411-17
- Du H, Zhang S, Song M, et al. Assessment of a flavone-polysaccharide based prescription for treating duck virus hepatitis. *PLoS One*, 2016;11:e0146046
- Zhi-Qiang H, Pan C, Wei-Wei S, et al. Antioxidant activity and hepatoprotective potential of quercetin 7-rhamnoside in vitro and in vivo. *Molecules*, 2018;23:1188
- Wimborne HJ, Takemoto K, Woster PM, et al. Aldehyde dehydrogenase-2 activation by Alda-1 decreases necrosis and fibrosis after bile duct ligation in mice. *Free Radic Biol Med*, 2019;145:136-45
- Zhang Z, Miao Y, Xu M, et al. Tianjiu therapy for  $\alpha$ -naphthyl isothiocyanate-induced intrahepatic cholestasis in rats treated with fresh *Ranunculus sceleratus* L. *J Ethnopharmacol*, 2020;248:112310
- Ommati MM, Amjadinia A, Mousavi K, et al. N-acetyl cysteine treatment mitigates biomarkers of oxidative stress in different tissues of bile duct ligated rats. *Stress*, 2020 [Online ahead of print]
- Zhao Y, He X, Ma X, et al. Paeoniflorin ameliorates cholestasis via regulating hepatic transporters and suppressing inflammation in ANIT-fed rats. *Biomed Pharmacother*, 2017;89:61-68
- Wang GW, Zhang XL, Wu QH, et al. The hepatoprotective effects of Sedum sarmentosum extract and its isolated major constituent through Nrf2 activation and NF- $\kappa$ B inhibition. *Phytomedicine*, 2019;53:263-73
- Zhou HQ, Liu W, Wang J, et al. Paeoniflorin attenuates ANIT-induced cholestasis by inhibiting apoptosis in vivo via mitochondria-dependent pathway. *Biomed Pharmacother*, 2017;89:696-704
- Wei S, Ma X, Zhao Y. Mechanism of hydrophobic bile acid-induced hepatocyte injury and drug discovery. *Front Pharmacol*, 2020;11:1084
- Yang JA, Kong WH, Sung DK, et al. Hyaluronic acid-tumor necrosis factor-related apoptosis-inducing ligand conjugate for targeted treatment of liver fibrosis. *Acta Biomater*, 2015;12:174-82
- Qi Z, Fang L, Cheng Y, et al. Celastrol protects from cholestatic liver injury through modulation of SIRT1-FXR signaling. *Mol Cell Proteomics*, 2019;18(3):520-33
- Khambu B, Li T, Yan S, et al. Hepatic autophagy deficiency compromises farnesoid X receptor functionality and causes cholestatic injury. *Hepatology*, 2019;69:2196-213
- Qiu X, Zhang Y, Liu T, et al. Disruption of BSEP function in heparg cells alters bile acid disposition and is a susceptible factor to drug-induced cholestatic injury. *Mol Pharm*, 2016;13(4):1206-16